CPW Fed Textile UWB Antenna for IoT and Wearable Applications

Mamta Devi Sharma*[1], Ajay Yadav[2], Sarthak Singhal[1], Ritu Sharma[1]

[1]Department of Electronics & Communication Engineering, MNIT, Jaipur, Rajasthan, India
[2] SP3 Technologies LLP, Surat, Gujarat, India

KEYWORDS
Circular Patch Antenna; I-shaped Slot; Textile Antenna; Specific Absorption Rate, Wearable Antenna, Internet of Things

Abstract: In this article, a compact circular shaped patch Ultra-Wide Band (UWB) antenna for Internet of Things (IoT) and wearable applications is presented. The proposed antenna incorporated a circular patch which excited by Coplaner Waveguide (CPW) fed line along with wide circular shaped and dual I-shaped slot in ground to improve the impedance bandwidth. According to presented analysis the designed textile antenna has wide impedance bandwidth i.e., approximately 17.2 GHz with maximum peak gain of 7.8 dB. The antenna has a compact size of 25x24 mm^2; it is simulated and fabricated on the Cordura textile substrate. The performance of the antenna in free space and on the human body phantom is presented in terms of impedance bandwidth, Specific Absorption Rate (SAR), and radiation characteristics. The SAR is calculated on a hypothetical body phantom at three different spots to validate the specified limits by international organizations for human safety. The maximum SAR values observed for 10 g average body mass are 0.258, 0.232, and 0.367 W/Kg, at the back side of the body, arm, and leg, respectively. The investigated results of the antenna in simulation and measurement are confirm its candidacy for IoT applications and body-worn devices.

1. Introduction

IN the current scenario, the demand for wireless communication systems increased; those can be utilized in the Internet of Things (IoT) for connectivity between biomedical sensing devices for exchange data, in the localization of movable targets, and in monitoring human health activities without any movement restriction [1]. Particularly, wireless wearable devices are highly appreciated after covid'19 pandemic to improve remote healthcare systems. These modern wireless devices support hospitals in transforming them into smart hospitals, and doctors can assess patients' vital signs remotely. So, IoT technology has been identified as one of the promising approaches that could fill the gap between the physical and virtual world by exchanging information from wearable sensors and electronic devices to smart clothes or smart accessories [2]. Existing and advanced IoT devices may need highly secure data transmission with a high-speed data rate without any major fading and interference. The antenna is a key element of wearable electronic and IoT systems that enable wireless communication between devices. However, the major problem with the existing single and multiband antennas is that they suffer from small bandwidth and high interference with the existing radio spectrum [3-4]. Most of them are fabricated with rigid substrates; they cannot be easily integrated into outfits and accessories.

*Corresponding author E-mail: 2019REC9017@mnit.ac.in, ajayrfmicrowave@gmail.com,sarthak.ece@mnit.ac.in,rsharma.ece@mnit.ac.in
Contact No. +91-9982804449
Address: Mamta Devi Sharma, Electronics and Communication Engineering, MNIT, Jaipur, Rajasthan 302017

So, the Ultra-Wideband (UWB) technology is extensively recognized for such required features due to high localization accuracy, reliable communication, low spectral power density, high data rate, resist interference with coexisting Radio Frequency (RF) devices, and ease of integration capability with other MMICs [5,6]. Moreover, due to low power emission, the impact of radiation on human tissue is almost negligible, and it is an emerging solution for data transmission between wearable devices and Wireless Body Area Network (WBAN) systems. Also, with investigations of flexible antenna designs, overcome the deformation mentioned above problem of the antennae with structure bending. In [7-8], authors designed monopole UWB antennas on very thin material, i.e., liquid crystal polymer (LCP) for wearable and IoT applications; in [9-10] used polyimide to design antennas for wearable and biomedical devices; in [11], the antenna has been fabricated on Polyethylene Terephthalate (PET), highly stretchable material PDMS and its composite used in [12-14] to develop the flexible antennas for wearable and IoT devices. Wearable textile antennas are gaining popularity because of their potential applications and merits. The textile antennas are suitable as an E-textile system for health care monitoring, navigation, rescue operations, and telemedicine; these can perform in different environmental conditions when bent and crumped with high robustness.

To enhance the comfort level and convenience of the wearer, various researchers have reported and proposed fabric-based antennas to achieve flexibility. For instance, in [15], authors proposed a fully textile UWB antenna printed on a jeans substrate for early-stage breast cancer detection. A textile sensor antenna has been investigated in [16] for self-monitoring and breast cancer detection. An antenna for healthcare applications has been fabricated on foam material, and a study reported on the performance of the structure in close proximity to human tissue [17]. A staircase with a rectangular patch antenna has been reported in [18], which is designed on denim textile and FR-4 for WBAN and IoT applications. Similarly, various textile antennas are investigated for wearable, IoT, and medical applications [19-21]. In [22], a circular slot with a defected ground plane on denim textile has been proposed, and in [23], a UWB antenna has been investigated for telemedicine applications on jeans material. To improve the impedance bandwidth and gain of the UWB antennas, wide slots in the ground plane are used [24-27]. However, these discussed antennas have disadvantages like large footprint [3] [5-20] and low gain [7-9][12-14][20][22-24]. The presented antenna overcomes the abovementioned issues; it provides high gain with a compact and simple structure.

The antenna design steps are detailed in Section 2, and the measured performance analysis of the antenna is discussed in Section 3. In section 4 and 5, the time domain analysis and the on-body performance of the antenna is discussed, and in section 6, the proposed research is concluded.

2. Antenna Design and Analysis

2.1 Antenna Fabrication and Design:

To design the flexible body-worn antenna, the textile material–Cordura is used, which has a dielectric constant (ε_r) = 1.9 and loss tangent $\tan\delta$ = 0.009, making it suitable for wide bandwidth, whereas the radiating element consists of self-adhesive copper tape. The low dielectric constant of Cordura supports diminishing the surface wave losses and increases the antenna operating bandwidth [28]. Due to the characteristics mentioned above, Cordura® fiber is found to be the most favorable and exciting fabric for the development of wearable textile antennas. The dimensional view of the designed wearable circular-shaped patch UWB antenna with circular-shaped slots in the ground is depicted in Figures 1 (a & b) and the fabricated prototype in Figure 1 (c). The conductive part of the fabricated antenna is cut in a specified shape using a Laser Cutting Machine. A 50-ohm SMA connector is attached to the antenna feed line and ground plane to measure the antenna characteristics. A low-power soldering machine with special glue is employed to secure the antenna connector. The circular patch is excited by a Coplanar Waveguide (CPW) fed line of width (W_f) =1.8 mm, and the gap (g) between the fed line and ground is 0.2 mm to achieve a reasonable impedance of 50 Ω.

The fabrication of textile-based antennas is highly challenging. If the metal part is adhered to the textile substrate by adhesive glue, then it can affect the durability of the antenna. To overcome this issue, self-adhesive copper tape is used for the proposed antenna fabrication. The second major challenge encountered is cutting copper tape in the required shape because the thin conductive tape cannot be easily cut by manual process, so to achieve the required geometry with good precision, a Laser Cutting Machine has been used. A low-temperature soldering iron is utilized to maintain the heat during SMA port soldering.

2.2 Antenna Evolution and Material Selection

The primary design, i.e., antenna-1 with a circular radiator and a wide circular slot of 20 mm diameter in the ground plane, resonated at the lower frequency of 4.3 GHz, as illustrated in Figure 2 by the dotted pink line. Furthermore, to achieve UWB band characteristics, one I-shaped slot of length L_1 is etched along with a circular slot in the ground plane at the upper side. However, the S_{11} is still above the -10 dB range from 6.3 to 9.3 GHz for antenna-2. Therefore, another slot of length L_2 is etched at the lower side in the ground to improve the reflection coefficient, as observed from the S_{11} plot of antenna-3 in Figure 2. However, impedance matching needs to be improved around 10 GHz. Furthermore, both slots are incorporated in the final proposed design to achieve a complete UWB band from 3.06 to 20.34 GHz.

The antenna suitability with other wearable substrates has been performed. Figure 3 shows the compared reflection coefficient and gain with different materials of the proposed structure, and it is found that Cordura provided slightly greater gain and good impedance in the entire working band. The peak gain is observed for felt, jeans, FR-4, and Cordura as 7.5, 6.8, 7.4, and 7.8 dB respectively.

2.3 Modeling of the Proposed Design

The suggested antenna reflection coefficient values are also validated by mathematical modeling, so an equivalent circuit is implemented using the CST circuit simulator, as shown in Figure 4. The equivalent circuit consists of two parts (i) a parallel combination of R_f (8.3 Ω) and L_f(330 pH) with C_f (0.038 pF) which denoted the values of fed line inductance and capacitance and (ii) six series resonate circuits. Each parallel combination has lumped elements of R_k, L_k, and at resonate frequencies in the UWB band. Where R_k, represents real impendence, L_k is inductance, and C_k is capacitance (k varies from 1 to 6) for the designed antenna at a resonate frequency. So, first consider impedance bandwidth and resonance frequency peaks for which impedance is near 50 ohms. The calculation for preliminary lumped elements i.e. R_k, L_k , and C_k, has been done using Equations (1-3) [29].

$$L_k = \frac{Im(Z_{11})}{2\pi f_k} \quad (1)$$

$$C_k = \frac{1}{(2\pi f_k)^2 L} \quad (2)$$

$$f_k = \frac{1}{2\pi\sqrt{LC}} \quad (3)$$

After that, values are tuned to obtain an approximate S_{11} graph as the proposed antenna shown above. The real and imaginary parts of the input impedance have been obtained by CST Microwave Studio software at six resonance frequencies i.e. 3.35 GHz, 4.88 GHz, 7.76 GHz, 10, 13.6 GHz, and 16.81 GHz in the UWB range of 3.04 GHz – 20.34 GHz. The tuned values of inductance and capacitance are summarized in Table 1 at different frequencies.

Figure 5, Demonstrates the comparison between the S_{11} extracted from CST and equivalent circuit results for the CST circuit simulator. As indicated in Figure 5, there is a slight shift between the results obtained due to tuning elements L_k and C_k.

2.4 Parametric Analysis of the Proposed Design

A parametric analysis has been carried out on slot length (L_1 and L_2) and diameter of circular ground slots (D_S) to find the optimized dimensions of the designed structure. The diameter of the slot (D_S) in the ground plane plays an important role in achieving wide-band operation. The parametric analysis of D_S is displayed in Figure 6. From Figure 6, it is noticed that the optimized value of the circular slot is 20 mm. By decreasing the diameter of the ground slot, the overall equivalent capacitance and inductance of the antenna vary, which reduces the impedance matching.

The asymmetrical I-slots in the ground also play an important role in achieving wide bandwidth and improved impedance matching for the proposed antenna structure. Figure 7(a) shows the effect on the reflection coefficient with variations of length L_1. Increasing slot length (L_1) improves the antenna impedance matching in the frequency range from 8.2 to 9.7 GHz band (which is achieved with the slot L_1as depicted in Figure 7(a).

Similarly, the length of the second slot (L_2) significantly influences the antenna performance from the 6 to 8 GHz frequency band. Increasing the value of L_2 improves the reflection coefficient of the structure, as demonstrated in Figure 7(b). The optimized value of slot length L_2 is 11 mm. The optimized perimeter of the ground slot is equal to πD_S+2L_1+2L_2+W_1+W_2. Properly optimizing the values of D_S, L_1, L_2, W_1, and W_2, can control the impedance bandwidth of the antenna and its resonance. The above parameter values decide the equivalent inductance values at a particular operation frequency.

3. Performance Analysis of the Textile Antenna

3.1 Reflection Coefficient and Gain Measurements in Flat Condition

After the calibration, the fabricated UWB antenna is measured by the KEYSIGHT Performance Network Analyzer (PNA-L N5234B). The simulated and measured reflection coefficient and gain of the fabricated textile antenna are depicted in Figure 8 and Figure 9, respectively. The variations between the simulation and measured S_{11} are observed due to the manufacturing tolerances in terms of copper sheet adhesion and SMA connector soldering.

3.2 Reflection Coefficient and Gain Measurements in Bending Condition

For a real scenario, the textile antenna may be stitched on garments, and in this situation, the structure may be bent on a curved body surface. The impedance matching of the antenna may change with the bending of the antenna. Also, the radiation characteristics would be affected by bending. Therefore, it is necessary to study the deformation effects on antenna performance. The proposed textile antenna curved at different radii and analyzed the reflection coefficient. Figure 10 represents the reflection coefficient values with different radii. The impedance matching differs at higher frequencies but within the operating band, giving satisfactory results up to a minimum radius of 30 mm.

However, the fabricated antenna parameters are evaluated after bending it on a cylinder surface of a minimum R = 30 mm radius, which is less than that of an adult human arm [30]. Figure 11 also shows the simulated and measured reflection coefficient in bent conditions. The gain measurement is done up to 18 GHz only due to measurement setup limitations. The textile antenna gain is ranged from 2 to 7.46 dBi in flat and bent conditions. It is observed from Figure 12 that the antenna gain has a good agreement between measured and simulated results in both conditions.

Table 2 summarizes the antenna performance in flat and different bending conditions. It can be noticed from this analysis that the antenna performs well after bending with slight variations in radiation characteristics and impedance characteristics.

3.3 Far-field Characteristics

Radiation characteristics of the antenna measured and simulated for flat and after bent at 30 mm radius (approximately 50^0 angles) conditions are presented for E-Plane (YZ plane) and H-plane (XZ plane) in Figure 13 and Figure 14, respectively. It is observed from Figure 13 (a to d) that the antenna provides a dipole-like shape at the lower frequencies, whereas it deviated at the higher frequencies due to the entry of higher-order modes in flat and bending conditions. In H-plane, the antenna shows the omnidirectional radiation pattern at lower frequencies in flat and bent conditions, and it is presented in Figure 14 (a to d). From Figure 13 and Figure 14, it is observed that the antenna has good radiation stability in bending conditions, and it follows the radiation just like the flat condition, so it can be a favourable candidate for the installation of various body parts without any significant deterioration in its radiation characteristics as reported in different studies [9][12][23][26]. Recently, some studies have analysed that the omnidirectional UWB antennas are suitable for IoT and WBAN applications and body-worn devices [14] [18][31-32].

3.4 Surface Current Distribution

The surface current distributions on the radiating element for the proposed antenna are shown in Figure 15 at the frequencies of 3.35, 7.76, 13.6, and 16.18 GHz. The electrical currents are mainly concentrated on the edges of the fed line and the ground plane. It is observed that the antenna has uniform current distribution at low as well as high frequencies, which validates that the antenna has good radiation stability.

4. Time Domain Analysis of the Proposed Antenna

The time domain analysis of the UWB antenna is a fundamental study to understand the short pulse communication behavior of the antenna. Through time domain analysis, designers and researchers examine the transient behavior of the antenna. Engineers acquire deep information about the directivity, gain, and efficiency of the antenna by observing how the radiated electromagnetic fields change with respect to time [33-34]. The group delay, fidelity factor, and system phase response are major performance parameters to examine the antenna in the time domain. For time domain performance analysis, two identical antennae were placed in the far-field region. They form a trans-receiver system; one works as a transmitter, and the other one as a receiver. To examine the time domain behaviour of the proposed structure, two identical antennae are placed in two configurations, i.e., face to face and side by side at a 150 mm distance. A Gaussian pulse is applied to the inputs of the antennas to excite them. The system fidelity factor (FF) is an important parameter to calculate signal integrity and cross-correlation between transmitted and received signals by using Equation (4) [35].

$$FF = max\left[\frac{\int_{-\infty}^{\infty} S_t\,(t).S_r(t+\tau)d\tau}{\int_{-\infty}^{\infty}|S_t(t)|^2 dt\,.\int_{-\infty}^{\infty}|S_r(t)|^2 dt}\right] \;\ldots\ldots\ldots\ldots\ldots\ldots.. \quad (4)$$

Where (t) and (t) are the transmitted signals and received signals, respectively, and is the group delay.

Figure 16 depicts the normalized amplitude of the transmitted signal and received signal, which indicates that the fidelity factor for face-to-face configuration is 90 %, and for side-by-side configuration, it is 78 %. A fidelity factor of more than 50%shows that there is less distortion in the received pulse.

The second important parameter of the UWB antennas is the group delay. Group delay is the negative ratio of change in phase of transmitted pulse to change in the frequency as expressed by Equation (5) [36]

$$\tau = -\frac{\partial \theta(\omega)}{\partial \omega} \quad \text{..................(5)}$$

Where τ is group delay in nanoseconds, (ω) is a phase of the transmitted signal, and ω is the frequency. The group delay of the proposed antenna is shown in Figure 17. The system has less than 1.2 ns group delay in both configurations, which indicates that the designed antenna is appropriate for wearable applications and IoT applications [35-36].

5. On-Body Performance

The textile antenna can easily stretch on the wearer's outfits to access or transmit data. The impedance and radiation characteristics of the antenna are influenced by body loading effects. Therefore, to investigate the impact of the body tissue on the antenna operation, the textile antenna is kept on a three-layer human phantom with dielectric properties taken from the CST library and at different body parts, i.e., the back side of the body, arm, and leg. The setup of the antenna analysis on human phantoms is depicted in Figures 18 (a & b), respectively. The dimension of the three-layer phantom is 100x100x23 mm^3. Figure 19(a) represents the textile antenna performance on a three-layer phantom with zero gap between the antenna and phantom. It is noticed that the proposed antenna is working on the entire UWB band on three layer phantom but the gain is reduced due to the high dielectric constant of the skin. Figure 19 (b) demonstrates the simulated and measured reflection coefficients in free space and when the structure is placed on the back side of the body, arm, and leg, respectively. It is observed that the measured operating bandwidth of the fabricated antenna from 4.18 to 20.4 GHz, on the arm and from 4.26 to 20.62 GHz, on the leg with some portion is slightly above − 10 dB. The variation in results with respect to the simulated one is due to the placing position of the testing antenna and the effective dielectric constant changed because of the extra fabric of the wearer. The reflection coefficient is measured by attaching the printed antenna on a 35-year-old female (without any gap between the antenna and the body) with cotton cloths.

Table 3 depicts the radiation characteristics of the proposed antenna in free space and with different human phantoms. It is clearly observed from Table 3 that the realized gain and radiation efficiency at different frequencies have been significantly reduced due to the lossy dielectric constant of the skin of the human body at lower frequencies. It is observed that the antenna performed well at higher frequencies as compared to low frequencies. At higher frequencies, the human body absorbs less EM power, and reflections are more. Due to that, the antenna radiates proficiently at higher frequencies.

SAR Evaluation: The SAR gives the value of Electromagnetic (EM) energy absorbed by human tissues [37]. It is expressed by Equation (6)

$$SAR = \frac{d}{dt}\frac{dw}{dm} = \frac{d}{dt}\frac{dw}{\rho dV} \text{ (W/Kg)} \quad \ldots\ldots\ldots\ldots\ldots\ldots\ldots\ldots (6)$$

Where dW shows the change in energy w.r.t time, dm is incremental mass, dV is the change in volume, and ρ presents the mass density. According to the IEEE C95.3 standard, SAR value must follow the safety rules and be below the specified criteria for humans, i.e., 1.6 W/kg over 1g tissue and 2 W/kg over 10 g tissue. At different frequencies, i.e., 3.34, 4.88, 7.76, 13.6, and 16.18 GHz, the simulated SAR distributions are summarized in Table 4 for 10 g and 1 g tissue by keeping the antenna 3 mm from the phantom (as set up shown in Figure18(b)).

The SAR distribution for 10g tissue at 3.35, 7.76, and 16.18 GHz frequencies are represented in Figure 20 (a to c) at the backside, arm, and leg, respectively. All values are within the specified limits by IEEE standards.

The proposed structure is compared with the recently investigated antennas in Table 5 in terms of size, operating bandwidth, gain, and SAR (for 10 g tissue). The reported designs have low gain as compared with this designed antenna. Furthermore, on-body analysis of the projected antenna shows stable performance by keeping the antenna near to the human body phantom, i.e., a 3 mm gap.

In the future, bandwidth can be enhanced up to 20 GHz by utilizing slot cutting in radiating parts and improving efficiency by using the embroidering process and metal deposition on nonconductive textiles. The directionality can be improved by using reflective surfaces with the antenna but at the compromise of the antenna profile. However, all these factors increase the complexity of the structure in terms of fabrication and cost. Although the embroidering method improves the flexibility and robustness of the antenna, it has less accurate geometry, and similarly, the printing method needs harmful chemicals, and ink can wear off over time.

In the coming years, textile antennas will replace bulky antennas in e-textiles within IoT and 5G networks. The designed textile monopole antenna can be utilized for various applications in the future, such as microwave imaging, tracking for personal safety, vital data transmission, and monitoring of sports persons.

The proposed design has the following salient features:

1. A simple geometry is proposed in this study with large operation bandwidth capability to cover the entire UWB spectrum from 3.1 to 10.6 GHz. The simplicity of structure reduces the fabrication complexity and overall structure volume as compared to Ref [7] [9] [14][16][22][31-35].

2. The designed antenna is fabricated on a textile substrate, which provides flexibility, low profile, lightweight, and can be easily integrated into wearable cloths and carry bags in contrast to semi-rigid substrates [3-8] and multi-stacked layers [19].

3. Obtained high gain and low SAR of the proposed design, making it more suitable for on-body applications and IoT applications.

6. Conclusion

In this research paper, a circular slotted textile antenna is designed and fabricated for wearable appliances. The antenna performs for wide bandwidth from 3.04 to 20.34 GHz with a maximum peak gain of 7.8 dBi at 19.3 GHz. The designed antenna shows consistent performance in air, after bending, and on the human body. The analyzed SAR values follow the IEEE standards with an input power of 50 mW. The maximum SAR obtained is 0.367 W/kg for 10g tissue. The proposed UWB antenna is a good candidate for wearable applications.

Acknowledgment

The authors are thankful to Government Women's Engineering College Ajmer (Raj.), India for felicitating the measuring facility for radiation pattern measurement in RF microwave lab and an anechoic chamber.

References

[1] Kalkhambkar, G., Khanai, R., and Chindhi, P. "A novel snail shell inspired wideband fractal antenna for internet of things applications", *Arab. J. Sci. Eng.*, **48**(11), pp. 15463-15474 (2023). doi.org/10.1007/s13369-023-08079-y.

[2] Atanasova, G. L., Atanasov, B. N., and Atanasov, N. T. " Fully textile dual-band logo antenna for IoT wearable devices", *Sensors*, **22**(12), pp. 4516 (2022). doi.org/10.3390/s22124516.

[3] Taksala Devapriya, A., and Robinson, S. "High gain compact wearable antenna for IoT applications", *Waves in Random and Complex Media*, pp.1-20 (2023). doi: 10.1080/17455030.2023.2266052.

[4] Kaur, K., and Kaur, A. "In silico, in vitro, and in vivo validation of a microwave imaging system using a low-profile ultra wide band archimedean spiral antenna to detect skin cancer", *Int. J. Imaging Syst. Technol.*, **34**(1), (2024).e23016. doi.org/10.1002/ima.23016

[5] Mahmood, S. N., Ishak, A. J., Ismail, A., and et al. " ON-OFF body ultra-wideband (UWB) antenna for wireless body area networks (WBAN): a review", *IEEE Access*, **8**, pp. 150844-63 (2022). doi: 10.1109/ACCESS.2020.3015423

[6] Kiani, S.H., Rafique, U., SAVCI, H.Ş., and et al. "Performance enhancement of vivaldi-shaped planar UWB antenna using a single-layer FSS reflector", *AEU-INT J Electron Commn.*, **178**, pp.155302 (2024). doi.org/10.1016/j.aeue.2024.155302

[7] Zahran, S. R., Abdalla, M. A., and Gaafar, A. " New thin wide-band bracelet-like antenna with low SAR for on-arm WBAN applications", *IET Microw. Antennas Propag.*, **13**(8), pp. 1219-1225 (2019). doi:org/10.1049/iet-map.2018.5801.

[8] Du, C., Wang, X., and Zhong, S. " A CPW-fed flexible ultra-wideband MIMO antenna based on liquid crystal polymer for IoT applications", *J. Electromagn. Waves Appl.*, **36**(15), pp.2198-2210, (2022). doi: 10.1080/09205071.2022.2070032,

[9] Reddy, B. N. B., Kumar, P. S., Rao, T. R., et al. "Design and analysis of wideband monopole antennas for flexible wearable wireless device applications", *Prog. Electromagn. Res. M*,**62**, pp. 167-174 (2017), doi.org/10.2528/PIERM17092107

[10] Dilruba Geyikoglu, M. "Novel UWB flexible antenna with dual notch bands for wearable biomedical devices", *Analog Integr. Circuits Signal Process.*, **114**(3), pp. 439-450 (2023). doi.org/10.1007/s10470-023-02146-y

[11] Hasan, M. R., Riheen, M. A., Sekhar, P., and et al. "Compact CPW-fed circular patch flexible antenna for super-wideband applications", *IET Microw. Antennas Propag.*,**14**(10), pp. 1069-1073 (2020). doi.org/10.1049/iet-map.2020.0155.

[12] Janapala, D. K., Nesasudha, M., Mary Neebha, T., and et al. "Design and development of flexible PDMS antenna for UWB-WBAN applications", *Wirel. Pers. Commun.*,**122**, pp. 3467–3483 (2022). doi.org/10.1007/s11277-021-09095-7

[13] Simorangkir, R. B., Kiourti, A., and Esselle, K. P. "UWB wearable antenna with a full ground plane based on PDMS-embedded conductive fabric", *IEEE Antennas Wirel. Propag. Lett*., **17**(3), pp. 493-496 (2018). doi: 10.1109/LAWP.2018.2797251.

[14] Meng, Q., Liu, X., Duan, J., and et al. "Ultra-wideband wearable antenna based on composite materials", *J. Mater. Sci.: Mater. Electron*., **34**(10), pp.861 (2023). doi.org/10.1007/s10854-023-10174-7

[15] Abdulla, F.A.a., and Demirkol, A. "A novel textile-based UWB patch antenna for breast cancer imaging", *Phys. Eng. Sci. Med*., **47**, pp. 851–861 (2024). doi.org/10.1007/s13246-024-01409-w

[16] Elsheakh, D. M., Alsherif, S. A., and Eldamak, A. R. "Textile monopole sensors for breast cancer detection", *Telecommun. Syst*., **82**(3), pp. 363-79 (2023). doi.org/10.1007/s11235-023-00990-x.

[17] Karad, K.V.,Hendre, V.S., Rajput, J.L.,and et al. "A SAR analysis of hexagonal-shaped UWB antenna for healthcare applications", *EURASIP J. Wirel. Commun. Netw*., **1**, pp.1-20 (2024).doi.org/10.1186/s13638-024-02405-0

[18] Mustaqim, M., Khawaja, B. A., Chattha, H. T., and et al. "Ultra-wideband antenna for wearable internet of things devices and wireless body area network applications", *Int. J. Numer. Model.: Electron. Netw. Devices Fields*, **32**(6), pp. 1-12 (2019). doi.org/10.1002/jnm.2590

[19] Yalduz, H., Tabaru, T. E., Kilic, V. T., and et al. "Design and analysis of low profile and low SAR full-textile UWB wearable antenna with metamaterial for WBAN applications", *AEU - Int. J. Electron. Commun*, **126**, 153465 (2020). doi.org/10.1016/j.aeue.2020.153465.

[20] De, A., Roy, B., Bhattacharya, A., and et al. "Bandwidth-enhanced ultra-wide band wearable textile antenna for various WBAN and internet of things (IoT) applications", *Radio Sci.*, **56**(11), pp. 1-16 (2021). doi.org/10.1029/2021RS007315

[21] Di Natale, A., and Di Giampaolo, E. "A reconfigurable all-textile wearable UWB antenna", *Prog. Electromagn. Res.* C, **103**, pp. 31-43 (2020).doi:10.2528/PIERC20031202

[22] Chen, P., Wang, D., Liu, L., and et al. "Design of UWB wearable conformal antenna based on jean material", *Int. J. Antennas Propag.*, pp. 1-12 (2022). doi:10.1155/2022/4886844.

[23] Yadav, A., Kumar Singh, V., Kumar Bhoi, A., and et al. "Wireless body area networks: UWB wearable textile antenna for telemedicine and mobile health systems", *Micromachines*, **11**(6), pp. 558 (2020). doi.org/10.3390/mi11060558

[24] Somasundaram, A., Thengalpalayam R.,S.K. and Alex, Z.C. "Development of wideband CPW fed microstrip patch antenna on textile substrate", *Microw. Opt. Technol. Lett*., **65**(8), pp.2352-2358. doi.org/10.1002/mop.33692

[25] Meena, M. L., Kumar, M., Parmar, G., and et al. "Design analysis and modeling of directional UWB antenna with elliptical slotted ground structure for applications in C- & X-bands", *Prog. Electromagn. Res.* C, **63,** pp. 193-207 (2016). doi:10.2528/PIERC16030804

[26] Varkiani, S. M. H., and Afsahi, M. "Compact and ultra-wideband CPW-fed square slot antenna for wearable applications", *Int. J. Electron. Commun*, **106**, pp.108–15 (2019). doi.org/10.1016/j.aeue.2019.04.024

[27] Jan, N.A., Kiani, S.H., Sehrai, D.A., and et al. "Design of a compact monopole antenna for UWB applications", *Comput. Mater. Contin*. ,**66**(1), pp.35-44 (2021). doi.org/10.32604/cmc.2020.012800

[28] Rafiq, M., Imran, A., Rasheed, A., and et al. "A review on the manufacturing techniques for textile based antennas", *J. Eng. Fibers Fabr*., **19**, (2024). doi.org/10.1177/15589250241226585

[29] Lodhi, D., and Singhal, S. "CPW fed quasi complementary super-wideband MIMO antenna", *Opt. Quantum Electron.*, **54**(12), pp. 808 (2022). doi.org/10.1007/s11082-022-04226-1

[30] Kanagasabai, M., Sambandam, P., Alsath, M. G. N., and et al. "Miniaturized circularly polarized UWB antenna for body centric communication", *IEEE Trans. Antennas Propag*., **70**(1), pp. 189-196 (2022). doi: 10.1109/TAP.2021.3098517

[31] Karad, K. V., and Hendre, V. S. "A flower bud-shaped flexible UWB antenna for healthcare applications", *EURASIP J. Wirel. Commun. Netw*., **2023**(1), pp. 1-8 (2023). doi.org/10.1186/s13638-023-02239-2

[32] Chen, P., Wang, D., and Gan, Z. "Flexible and small textile antenna for UWB wireless body area network", *Micromachines*, **14** (4), pp. 718 (2023). doi.org/10.3390/mi14040718

[33] Kiani, S.H., Savci H.S., Munir M.E., and et al. "An ultra-wide band MIMO antenna system with enhanced isolation for microwave imaging applications", *Micromachines*, **14**(9), pp.1732 (2023). https://doi.org/10.3390/mi14091732

[34] Savci, H.¸S. "A four element stringray-shaped MIMO antenna system for UWB applications", *Micromachines*, **14**, pp. 1944 (2023). doi.org/10.3390/mi14101944

[35] Khan, M.A., Rafique U, Savci H.Ş., and et al. "Ultra-wideband pentagonal fractal antenna with stable radiation characteristics for microwave imaging applications", *Electronics*, **11**(13), pp. 2061 (2022). doi.org/10.3390/electronics11132061

[36] Karad, K.V. and Hendre, V.S. "A hexagonal shape fractal flexible UWB antenna based on jeans material for healthcare applications", *J. Text. Inst.*, pp.1-16 (2024). doi.org/10.1080/00405000.2024.2372954

[37] Sharma M.D., Yadav A., Singhal S., and et al. "Performance investigation of flexible UWB antenna near human body for wearable appliances", *Prog. Electromagn. Res. B*, **97**, pp. 131-147 (2022). doi:10.2528/PIERB22101109.

FIGURES CAPTIONS LIST

TABLE CAPTIONS LIST

FIGURES

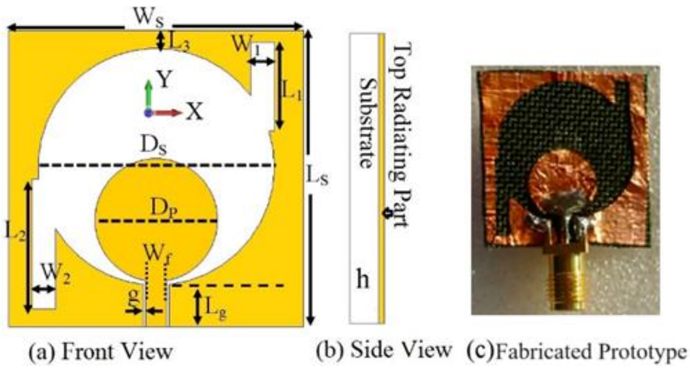

Figure 2. Geometrical configuration (a) Front View (b) Side View (c) Fabricated Prototype (W_S = 24, L_S = 25, W_f= 1.8, L_f =3.38, g = 0.2, D_S=20, D_P=10.4, W_1= W_2= 2, L_1 = 7.5 L_2 = 11 and L_3 = 1.5 (all dimensions in mm)).

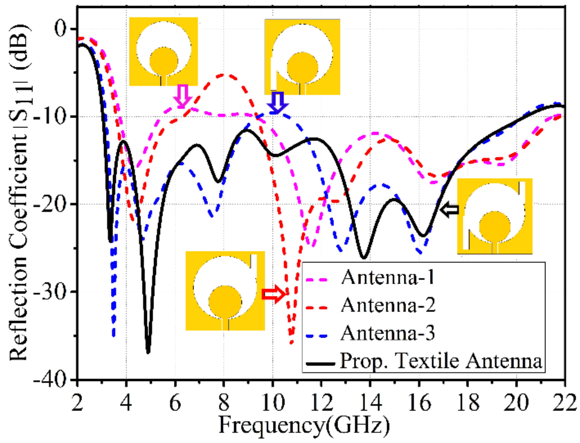

Figure 2. Reflection coefficient of different steps

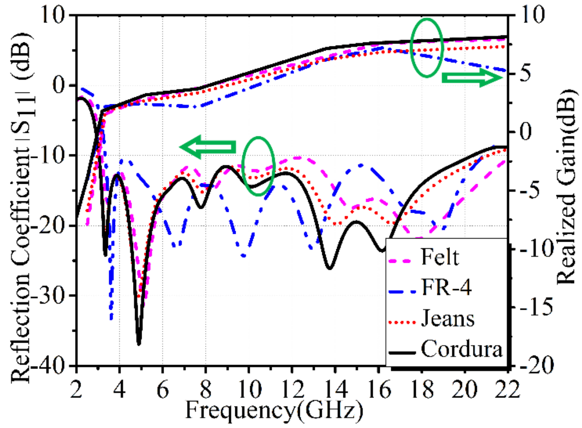

Figure 3. Reflection coefficient and gain of the antenna with different dielectric substrate materials

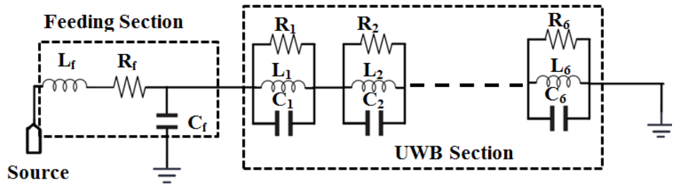

Figure 4. Electrical equivalent circuit of the designed antenna

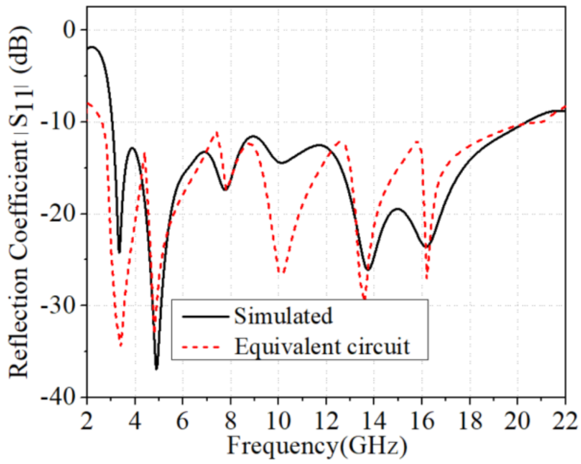

Figure 5. Reflection Coefficient plot of CST and equivalent circuit

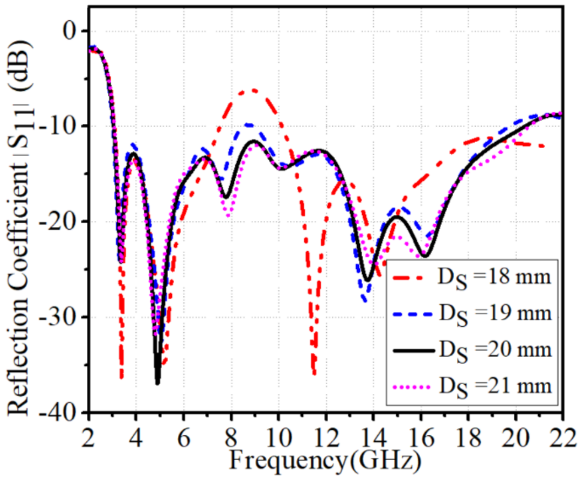

Figure 6. Parametric study of circular slot diameter (D_S) variation on the reflection coefficient

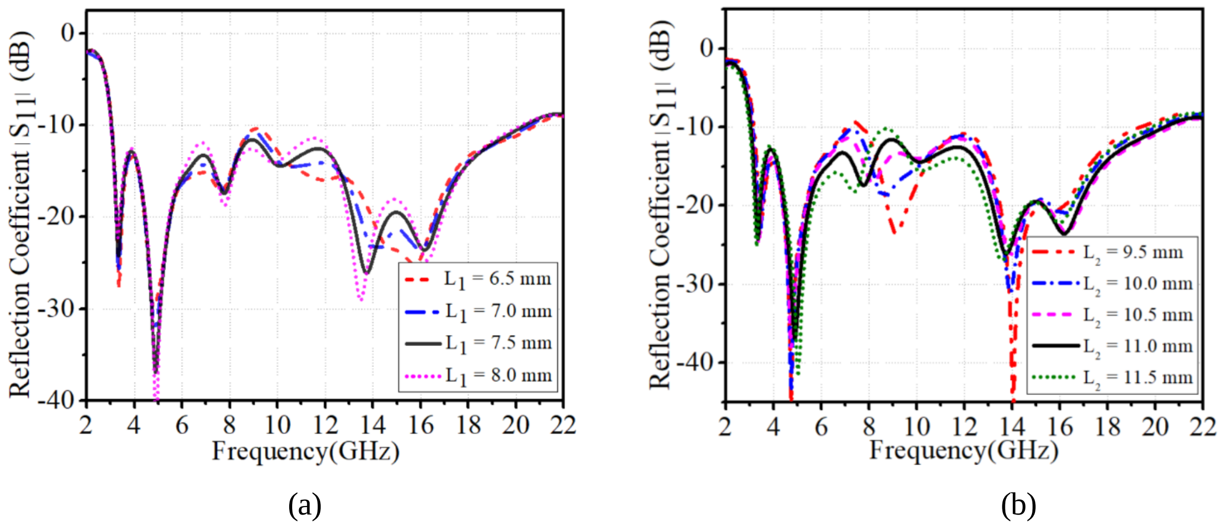

Figure 7. Parametric study reflection coefficient with slot length (a) L_1 and (b) L_2

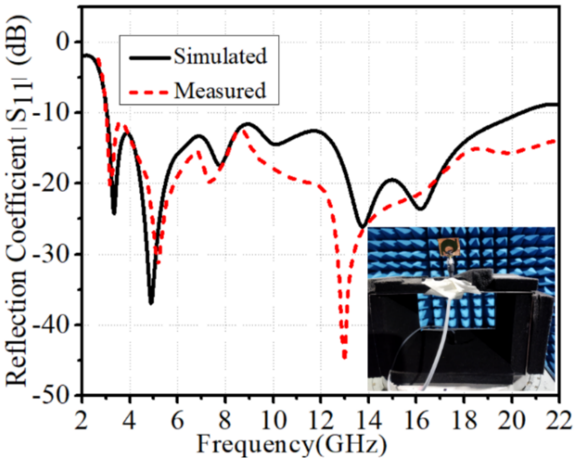

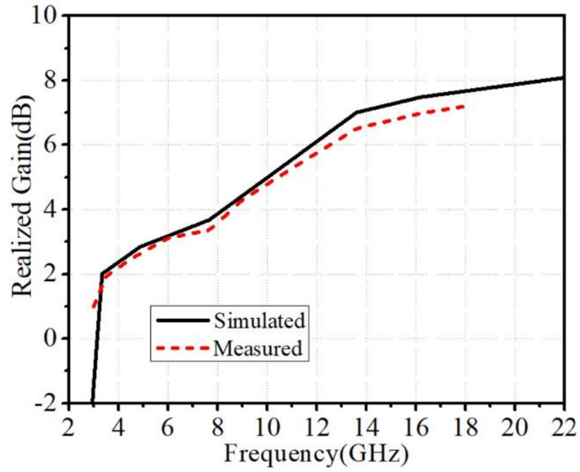

Figure 8. Measured and simulated reflection coefficient

Figure 9. Measured and simulated gain plot

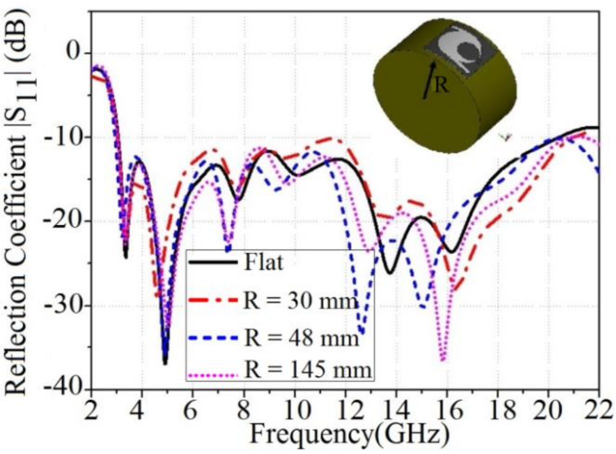

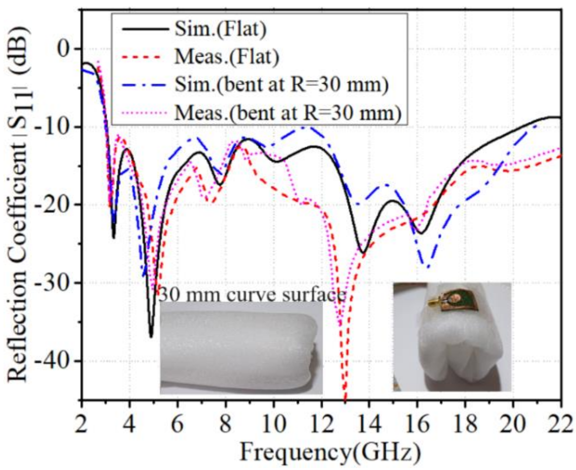

Figure 10. Reflection coefficients at different radii

Figure 11. Simulated and measured reflection coefficient with bending

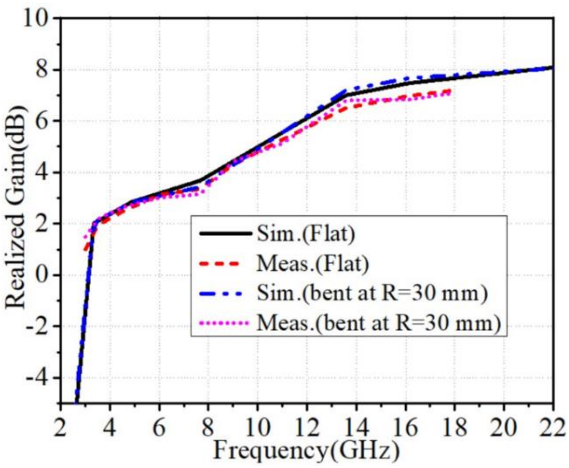

Figure 12. Simulated and measured gain with bending

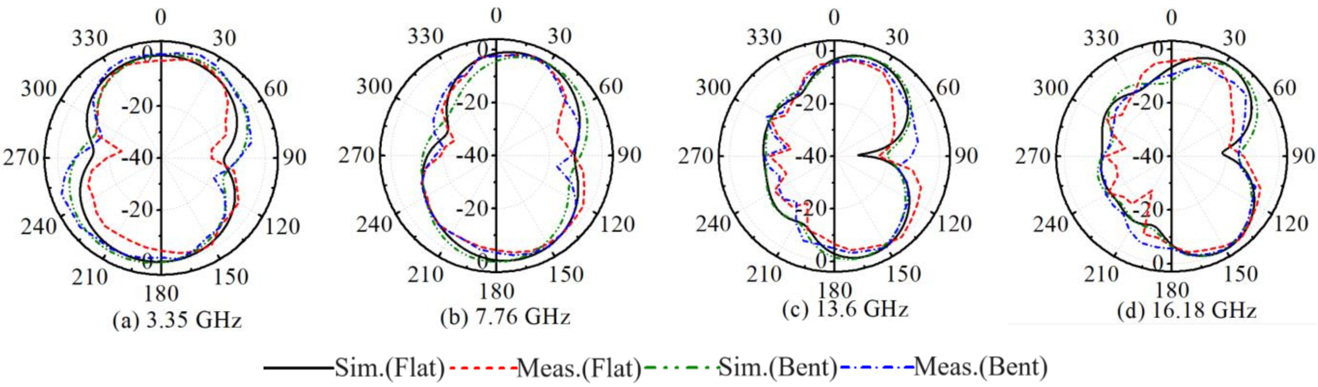

Figure 13.Simulated and measured radiation patterns in E- plane

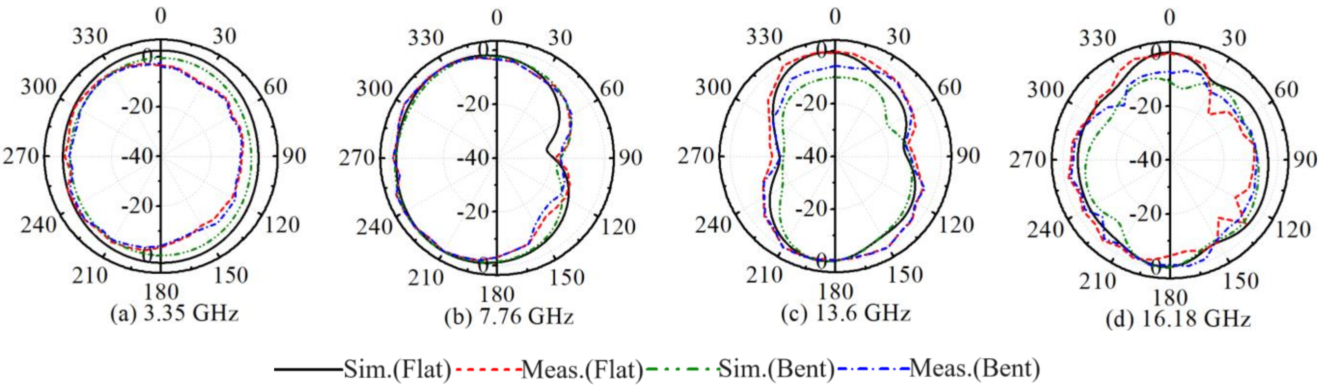

Figure 14. Simulated and measured radiation patterns in H- plane

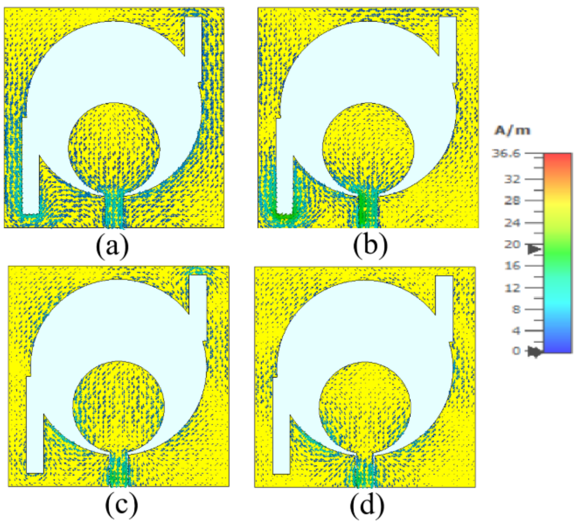

Figure 15. Current distribution at (a) 3.35 GHz, (b) 7.76 GHz, (c) 13.6 GHz, and (d) 16.18 GHz

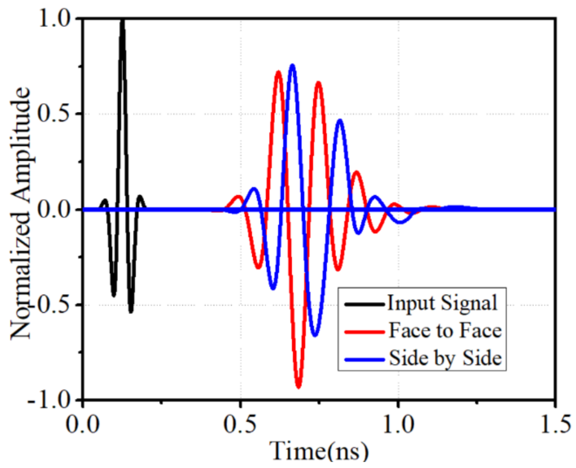

Figure 16. Pulse response of the proposed antenna in the time domain

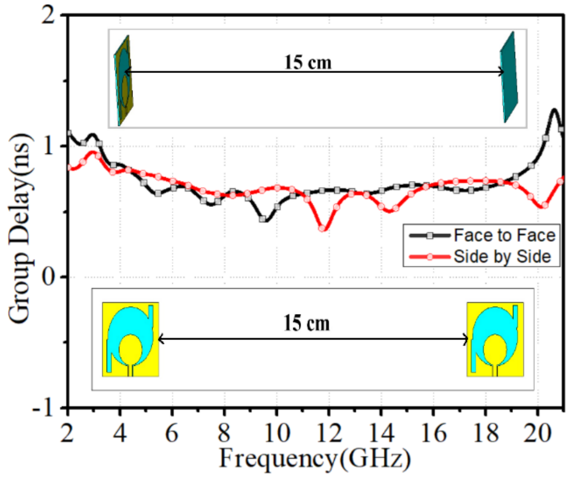

Figure 17. Group delay of the proposed antenna

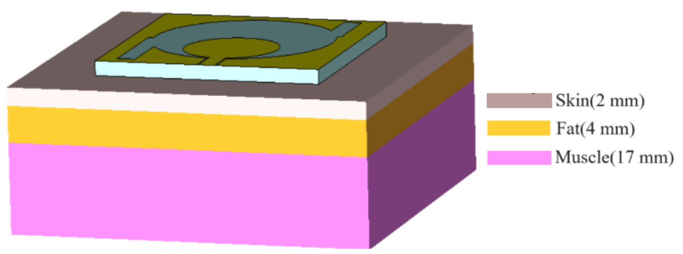

Figure 18 (a). Antenna set up on three-layer phantom

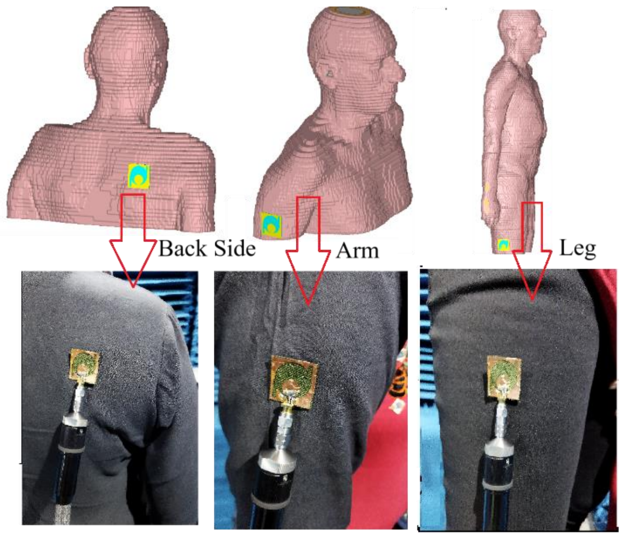

Figure 18 (b). Antenna test set up with human body parts

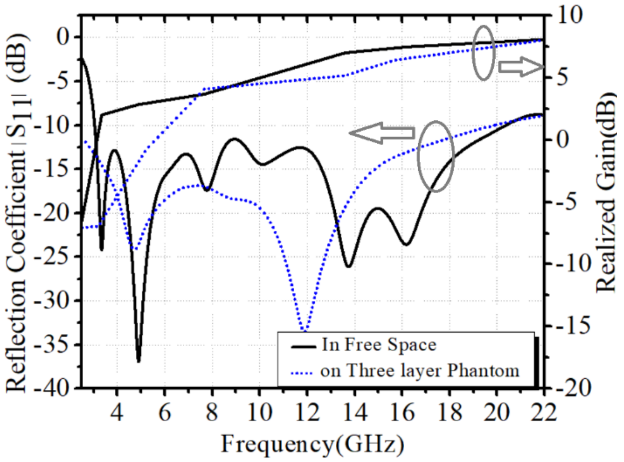

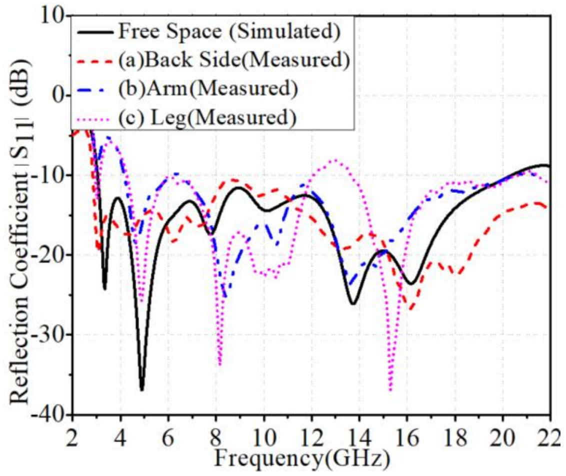

Figure 19 (a). Proposed antenna performance with three-layer phantom

Figure 19 (b). Proposed antenna performance on different body sites

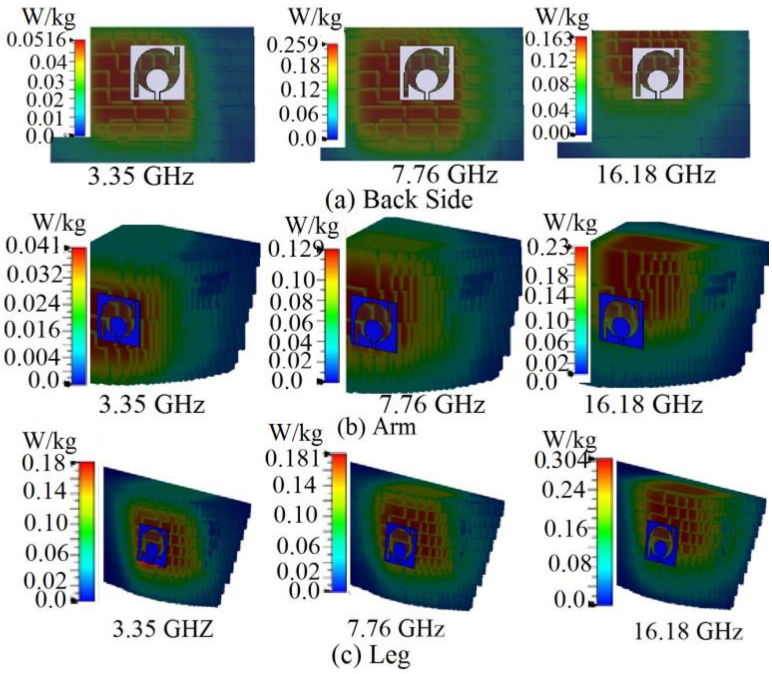

Figure 20. SAR distribution at different body parts

TABLES

Table 1. Equivalent Circuit Parameters Values of Antenna

k	Frequency (GHz) (f_k)	Z_{11} (Ω)		L_k (pH)	C_k (pF)
		Real (R_k)	Imaginary (X_k)		
1	3.35	53.98	-5.023	579	3.89
2	4.88	51.34	-0.5395	32.8	32.4
3	7.76	64.65	4.92	39.8	10.5
4	10	73.41	-0.475	73.4	3.45
5	13.6	55.04	-2.11	15.2	9.00
6	16.18	55.03	4.816	4.43	21.8

Table 2. Antenna Performance in Flat and Bending Condition

Configuration	**Bending w.r.t to radius**	**Operating Band (GHz)**	**Peak Gain (dBi)**
Flat	0^o	3.06 - 20.34	7.46
Bending on R=145 mm	10^o	2.95 - 20.42	7.8
Bending on R=48 mm	30^o	2.9 - 20.38	7.7
Bending on R=30 mm	50^o	2.93 - 20.87	7.6

Table 3. Gain of the Proposed Antenna in various Conditions

Frequency (GHz)	**Realized Gain in dBi**			**Radiation Efficiency (%)**	
	Free Space	**Three Layer Phantom**	**Arm**	**Free Space**	**Three Layer Phantom**
3.35	2.02	-5.8	-6.2	99	10
7.76	3.67	4.08	3.5	78	25
13.6	7.00	5.17	5.8	94	35
16.18	7.4	6.54	6.9	95	40

Table 4. SAR Analysis on Different Body Sites

Frequency (GHz)	**Back Side**		**Arm**		**Leg**	
	10g	**1g**	**10g**	**1g**	**10g**	**1g**
3.35	0.0516	0.1333	0.0410	0.0787	0.180	0.3020
4.88	0.0688	0.1284	0.0841	0.1450	0.102	0.1623
7.76	0.2589	1.1623	0.129	0.2500	0.181	0.4184
13.6	0.1818	0.5415	0.214	0.6390	0.367	1.2190
16.18	0.1629	0.5735	0.232	0.6066	0.304	0.6501

Table 5. Comparison between Recently Reported and Proposed Work

Ref [ ]	Size (mm^3)	Material(ε_r)	Band (GHz)	Max Gain (dBi)	Max SAR (W/Kg)
[6]	20 x 27 x 1.6	FR-4(4.4)	3.1 -20	4.55	NA
[7]	51x22x0.1	LCP(2.9)	2.4-3.5& 5.4-10.4	2.2(Avg)	0.966
[9]	50x40x0.8 50x40x0.712	Polyamide(4.3) Teslin Paper(2.23)	1.8-13.3 1.45-13.4	5.53 4.4	0.52 0.75
[14]	60x50x0.5	PDMS/BaTiO3/PTFE (2.8)	2-13	2.88 dB	1.28
[16]	50 x 50 x 2	Cotton (1.6)	2.2-8	4(Avg)	0.174
[19]	80 x61 x 1	Felt(1.4)	4.55 -13	6	0.107
[20]	45x33x1.75	Denim(1.78)	2.40-14.8	6.7	NA
[22]	20x30x1.4	Jeans(2.2)	2.9-10.6	3.03	1.86
[27]	26 x 25x1.6	FR-4	3.2 -12.0	4 dB	NA
[30]	25x30x1.4	Jeans(1.7)	3.09-11	2.3-4.4	1.02
[31]	38x30x1.7	Foam(10.7)	2.6-11.3	5.24dB	1.23
[32]	20x30x1.4	Jeans(2.2)	2.85–9.81	3.28	1.29
[33]	26x28x0.787	Roger RT/Duroid 5880 (2.2)	3.2-11.5	5.9	NA
[34]	26x29x0.787	Roger RT/Duroid 5880 (2.2)	3.8-12	3.7	NA
[35]	24×30×0.787	Roger RT/Duroid 5880 (2.2)	3-12.7	3.6	NA
***	25x24x0.5	Cordura (1.9)	3.04 - 20.34	2-7.46	0.232

NA: Not Available *** In proposed work

Biography

Mamta Devi Sharma received a B.E degree in 2006 in Electronics and Communication Engineering from Rajasthan University, Jaipur, and M. Tech. from RTU Kota, Rajasthan, in Digital Communication Systems in 2012. She is currently pursuing a Ph.D. degree in Electronics and Communication at Malaviya National Institute of Technology (MNIT), Jaipur, Rajasthan, India, and working as a Junior Research Fellow. She has 16 years of academic experience as an assistant professor. Her area of research interest includes the design and analysis of planar UWB Antenna, RF/Microwave filters, Conformal Antennas, Phased Array Antenna, UWB Antennas for biomedical applications, LNA, Oscillators, power dividers, splitters, Meta materials, Frequency Selective Surfaces, Reconfigurable antennas, and Tera Hertz Communication. She has published more than 15 research papers in International/National conferences and peer reviewed International Journals.

Dr. Ajay Yadav received a B.Tech (AMIETE) degree in Electronics and Telecommunication from IETE, New Delhi, India, in 2008 and an M.Tech. degree in Microwave Electronics from the University of Delhi, India, in 2011. He completed a Ph.D. degree in Electronics and Communication from Malaviya National Institute of Technology (MNIT) in 2020, Jaipur, Rajasthan, India. Currently working in the industry in R&D Dept. He has published more than 50 research papers in International/National conferences and peer-reviewed International Journals. He has authored 3 books and 4 book chapters for national and international publishers. He is a Senior Member of IEEE and a Life Member of IETE. He has more than 14 Years of experience in Industries (Embedded systems and RF/Microwave) and Academia. He has supervised 6 M. Tech dissertations and is also the winner of the “Chhatra Vishwakarma Award 2019” as a Mentor. He has also completed a sponsored Project on Bio-degradable RFID Tags. His area of research interest includes the design and analysis of planar antennas, RF/Microwave filters, Conformal

Antennas, Phased Array Antenna, UWB Antenna, LNA, Oscillators, power dividers, splitters, Metamaterials, Frequency Selective Surfaces, Reconfigurable antennas, Tera Hertz Communication.

Sarthak Singhal was born in Gwalior (MP) in 1987. He received his BE degree in Electronics & Telecommunication Engineering from SGSITS, Indore (MP) in 2010, the M. Tech degree in Microwave Engineering, and the PhD degree from IIT (BHU) Varanasi in 2012 and 2015, respectively. He worked as an Assistant Professor at Amity School of Engineering & Technology (ASET), Bijwasan, New Delhi, Amity University, Gwalior (MP) and Madhav Institute of Technology & Science, Gwalior (MP). Presently, he is an Assistant Professor at Malaviya National Institute of Technology, Jaipur, since February 2019. He has published over 76 research papers in journals, 29 in conference proceedings, and 2 books titled "Design and Analysis of Shorted Gap Coupled Patch Antenna" and "Design and Analysis of Ultra Wideband Microstrip Antennas" from LAPLAMBERT Academic Publishing House. His research interest includes the areas of design of millimeter frequency antennas, dielectric resonator antennas, microstrip antennas, EBG, artificial magnetic conductors, soft and hard surfaces, phased array antennas, and computer-aided design for antennas.

Ritu Sharma, completed her bachelor of engineering from Jai Narayan Vyas University, Jodhpur, in 1994. She has completed her Master's in Electronics and Communication Engineering and Ph.D. Degree in the field of photonics from Malaviya National Institute of Technology, Jaipur, in 2004 and 2011 respectively. She worked at Modi Olivetti Ltd., Bombay, and Technomics Pvt. Ltd., Bombay, as a work controller for 1 year. Presently, she has been an Assistant Professor in the Department of Electronics and Communication, Malaviya National Institute of Technology, Jaipur, since 1999. She has supervised 10 Ph.D. dissertations and several M.Tech thesis in the field of MEMS-based sensors, Communication, and Nanotechnology. Her research area includes photonics, superconductivity, MEMS, and nanotechnology.